JOURNAL OF SOLID STATE CHEMISTRY 90, 47–53 (1991)

Structural Study of Peroxopolytungstic Acid Prepared from Metallic Tungsten and Hydrogen Peroxide

TOKURO NANBA,* SANAE TAKANO, ITARU YASUI, AND TETSUICHI KUDO

Institute of Industrial Science, University of Tokyo, Roppongi, Minato-ku, Tokyo 106, Japan

Received June 15, 1990, in revised form August 13, 1990

The structure of peroxotungstic acid (W-PTA) prepared from metallic W and aqueous H_2O_2 was investigated based on Raman, IR, and XRD analyses. W-PTA was an amorphous compound constructed of peroxo polytungstate anions, in which the anions were bound to each other through hydrogen bonding. RDF analyses suggested that the polyanion was $W_{12}O_{38}(O_2)_6^{16-}$, in which a six-membered ring of corner-shared polyhedra, such as $WO_5(O_2)$ or WO_6, was sandwiched by two W_3O_{10} units consisting of edge-shared WO_6. © 1991 Academic Press, Inc.

Introduction

One of the present authors reported that peroxotungstic acid (PTA) could be prepared using the reaction of H_2O_2 with metallic tungsten (W-PTA) and tungsten carbide (WC-PTA) (*1*). PTA is amorphous and has a high water solubility, from which thin films can be easily formed. It has also been reported that the films prepared from W-PTA showed promising electrochromic properties. From W-PTA and WC-PTA some crystalline salts can be derived together with Ba^{2+}, Cs^+, K^+ 18-crown-6, etc. (*2*); structural studies have been performed (*3, 4*) on these materials. It has been thought that W-PTA and WC-PTA had structures similar to that of the K^+ 18-crown-6 salt, $[K(C_{12}H_{24}O_6)]_4(CW_{12}O_{40})$, in which the $(CW_{12}O_{40})^{4-}$ polyanion had a distorted Keggin-type structure (*4*). As for the starting materials, W- and WC-PTA, detailed structural analyses have not been carried out. In this study we examined the structure of W-PTA using IR, Raman spectroscopic studies, and a radial distribution analysis.

Experimental

Metallic W powder (8 g) was added little by little to a 15% H_2O_2 aqueous solution (50 ml). After filtration of the unresolved impurities and decomposition of the excess H_2O_2 with a Pt black net, the solution was rapidly condensed and pale yellow particles of W-PTA were obtained. The powdered W-PTA was used for the following analyses.

Quantities of peroxo group O_2^{2-} and the involved water were determined with an iodometric titration and by thermogravimetric analyses (TGA).

The density was measured by a pycnome-

*Present address: Faculty of Engineering, Okayama University, Tsushimanaka, Okayama-shi 700, Japan.

0022-4596/91 $3.00

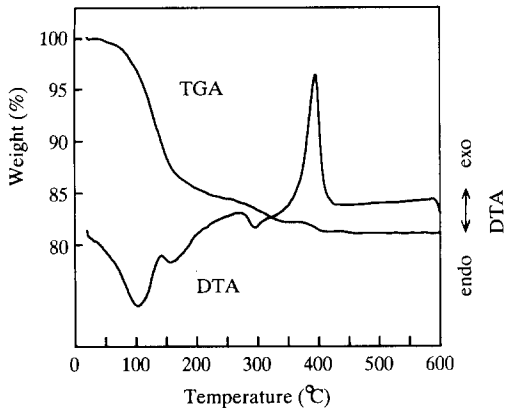

FIG. 1. TGA and DTA curves of W-PTA.

ter method in benzene. IR spectra were obtained from KBr pellets, and Raman spectra were measured with a JASCO R-800 spectrometer at a scattering angle of 90°, a wave length of 4880 Å, and a power of 3 mW. XRD measurements were carried out with a step-scanning method for 300 ~ 600 sec of fixed counting time. A MoK_α radiation with an output of 60 kV–150 mA was monochromatized with Zr–Y-balanced filters, a graphite monochromator in a diffracted beam, and a pulse height analyzer. The radial distribution function was obtained via the usual methods.

Results and Discussion

1. Composition and Some Properties

The results of TGA and a differential thermal analysis (DTA) are shown in Fig. 1 (heating rate = 20°C/min). Three steps of weight loss were observed at RT ~200°C, 250 ~ 330°C, and 370 ~ 400°C. These losses were mainly assigned to dehydration. Three endothermic and one exothermic peak, which were attributed to the dehydration of involved water and to crystallization, respectively, appeared in the DTA curve.

W-PTA was heat-treated at 100, 150, 200, 240, 350, and 450°C for 1 hr. XRD measurements were carried out (fixed time = 10 sec) to judge the degree of crystallinity of the samples. The obtained profiles are shown in Fig. 2. The samples were amorphous below 200°C, and a crystalline phase was observed at 240°C. Above 350°C the samples were completely crystallized. The crystalline phase was assigned to monoclinic WO_3. A broad peak seen at $2\theta = 4°$ shifted to lower positions as the heat-treatment temperature became higher. This fact suggested that the as-prepared W-PTA consisted of micro-voids and -clusters (polyanions).

The analyzed composition and density are listed in Table I, together with those of the heat-treated derivatives. Peroxo groups were present only in the as-prepared W-PTA, and water was commonly involved in

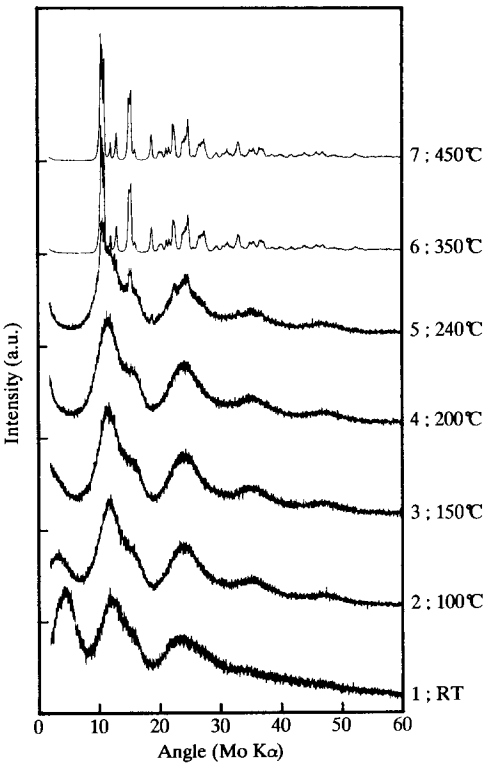

FIG. 2. XRD profiles of the as-prepared W-PTA and the post-annealed samples.

TABLE I

ANALYZED COMPOSITIONS AND DENSITIES AND COORDINATION NUMBERS OF THE NEAREST NEIGHBORING W–W PAIRS (*Nco*) IN THE NEIGHBORING STRUCTURAL UNITS SHARING THEIR CORNERS AND EDGES

Sample No.	Heat-treatment temperature (°C)	Composition		Density (g/cm³)	*Nco*	
		O_2^{2-}/W	H_2O/W		Corner (3.72Å)	Edge (3.22Å)
1	RT	0.6	1.8	3.7(4)	3.1	1.0
2	100	0.0	1.1	5.1(4)	4.5	0.5
3	150	0.0	0.5	5.3(9)	4.8	0.3
4	200	0.0	0.4	5.7(2)	5.0	0.2
5	240	0.0	0.2	6.3(4)		
6	350	0.0	0.0	7.0(6)		
7	450	0.0	0.0	7.2(6)		

the amorphous samples. Two endothermic peaks were observed below 200°C in the DTA curve, RT ~150°C and 100 ~200°C, and the peroxo groups disappeared in the sample heated at 100°C. It is therefore suggested that the first peak is due to the dehydration; the second one is assigned not only to dehydration but also to the decomposition of the peroxo groups.

The density increased along with the heat-treatment. This result supports the previous view that W-PTA contains microclusters.

2. *IR and Raman Spectra*

In Fig. 3 the IR spectrum of W-PTA is shown together with the results of the heat-treated derivatives. As the temperature became higher, the absorptive peaks around 1600, 960, and 550 cm^{-1} became smaller. These peaks are assigned to the vibrations of OH, terminal W=O, and WO_2, including the peroxo group (*5*, *6*), respectively. The other broad peaks between 900 and 600 cm^{-1} are attributed to the W–O stretching modes in the networks of WO_6 octahedra (*5*).

Raman spectra are shown in Fig. 4. The peaks of W=O were commonly seen in the amorphous samples heat-treated below 350°C. The broad peaks around 700 ~ 800 cm^{-1} in the samples heated at 100 ~ 240°C could be deconvoluted in two peaks at 800 and 700 cm^{-1}, which sharpened in the crystallized samples. The Raman profiles of the crystallized samples were the same as that of monoclinic WO_3. The spectrum of W-PTA showed a different profile from other samples; the intensity around 900 ~ 600

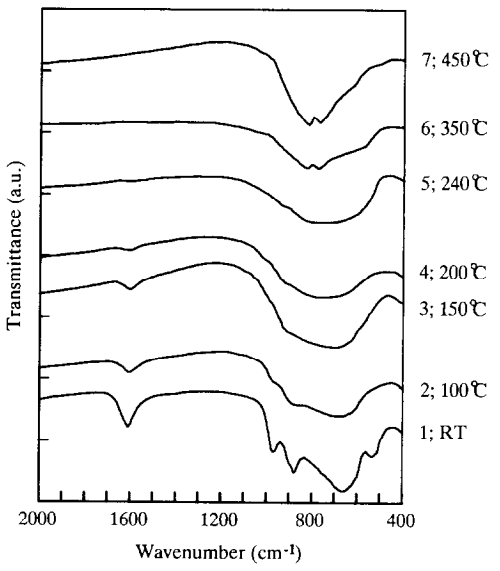

FIG. 3. IR spectra of W-PTA and the post-annealed samples.

TABLE II

VIBRATIONAL FREQUENCIES (cm^{-1}) IN SOME TUNGSTEN OXIDES, HYDRATES, AND A PEROXOTUNGSTATE GIVEN BY DANIEL *et al.* (*5*) AND GRIFFITH *et al.* (*6*)

Group	Monoclinic WO_3	Hexagonal WO_3	$WO_3 \cdot 2H_2O$	$WO_3 \cdot H_2O$	$WO_3 \cdot 1/3H_2O$	$K_2W_2O_{11} \cdot 4H_2O$
	Three-dimensional networks		Two-dimensional networks		Three-dimensional networks	Two-membered pentagonal bipyramids
W=O			960	948	945	958[a]
O–O						850[a]
	807	817			805	
W–O	715	690	685		680	
		645	662	645		
						563[a]
$W(O_2)$						530[a]

[a] Given by Griffith and Wickins (*6*).

cm^{-1} was very weak, and the peaks at 950 and 550 cm^{-1} not observed in the post-annealed samples were assigned to vibrations of peroxo groups in $W(O_2)$ (*6*). Some Raman bands of tungsten trioxides, its hydrates, and a peroxotungstate are summarized in Table II. The peak positions of W-PTA are mostly in agreement with those of $K_2W_2O_{11} \cdot 4H_2O$, whose structural units were pentagonal bipyramids of $WO_2(O_2)_2(OH_2)$ (*7*).

We consequently concluded that three-dimensional networks formed by WO_6 octahedra were constructed in the heat-treatment. On the contrary, the as-prepared W-PTA had lower dimensional networks or lower symmetrical octahedra forming three-dimensional networks. However, it was obvious that W-PTA contained WO_7 pentagonal bipyramids such as $WO_2(O_2)_2(OH_2)$.

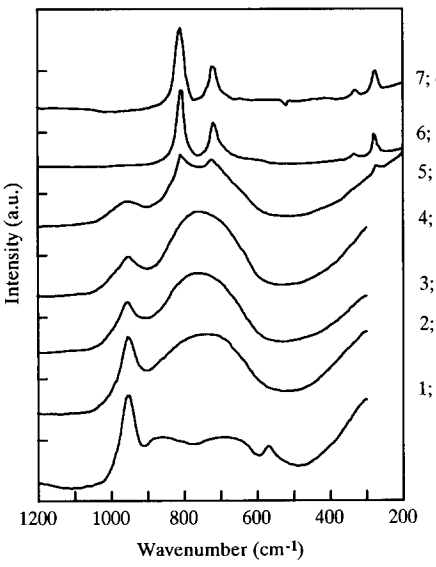

FIG. 4. Raman spectra of W-PTA and the post-annealed samples.

3. Radial Distribution Functions

The RDFs of the amorphous samples are shown in Fig. 5. Two main peaks were observed at 2 and 3.7 Å, and were attributed to the nearest neighbors of W–O and W–W, respectively. The peaks were located at almost the same positions in all samples. Accordingly, it was found that the basic structure formed in the as-prepared W–PTA was maintained even in the postannealed samples. The peaks at $R > 4$ Å are mainly affected by W–W; the peak around $5 \sim 6$ Å is assigned to W–W, which is located at opposite corners in the four-membered rings formed by WO_6 or WO_7 polyhedra, and the peak at 7 Å is attributed to W–W in six-

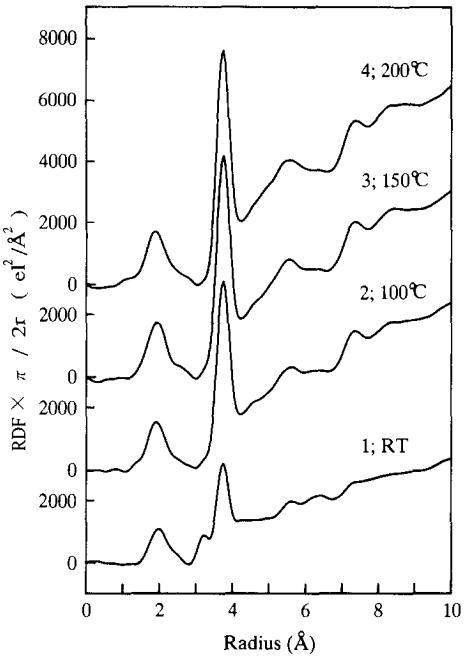

FIG. 5. Observed RDFs of W-PTA and amorphous heat-treated samples.

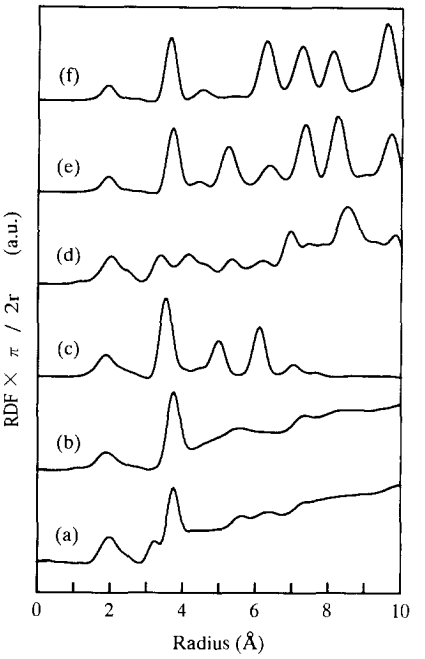

FIG. 6. Comparison between the observed and the calculated RDFs. (a) W-PTA; (b) heated at 200°C; (c) $[K(C_{12}H_{24}O_6)]_4(CW_{12}O_{40}) \cdot 2H_2O$; (d) $K_6[W_4O_8(O_2)_6(CO_3)] \cdot 6H_2O$; (e) Ba_xWO_3, (f) Cs_xWO_3.

membered rings. The post-annealed specimens showed RDF profiles similar to that of the vacuum-evaporated WO_3 film (*8*). This suggests that the networks of six-membered polyhedra are present in W-PTA and its heat-treated derivatives.

One small peak at 3.2 Å was present in W-PTA; it almost disappeared in the heat-treated samples. This peak can also be assigned to the nearest neighboring W–W, which is the pair in the neighboring WO_6 or WO_7 polyhedra sharing their edges. The large peaks at 3.7 Å are due to the corner-shared polyhedra. A deconvolution was performed for the second peak by means of a pair-function method; we obtained the averaged coordination number of the nearest W–W pairs (*Nco*) as listed in Table I. As the heat-treatment temperature became higher, the *Nco* (edge) decreased but the *Nco* (corner and total) increased. These results lead to the following suggestions: W-PTA and the amorphous samples contained a greater number of edge-shared polyhedra and exhibited a larger termination of networks. In the crystallized samples, the edge-shared polyhedra disappeared and continuous networks were built.

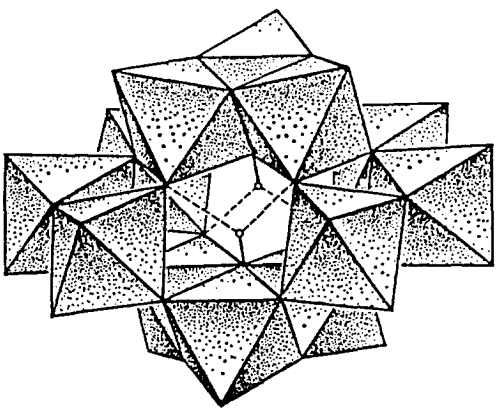

FIG. 7. Structure of "paratungstate-B" (*11*).

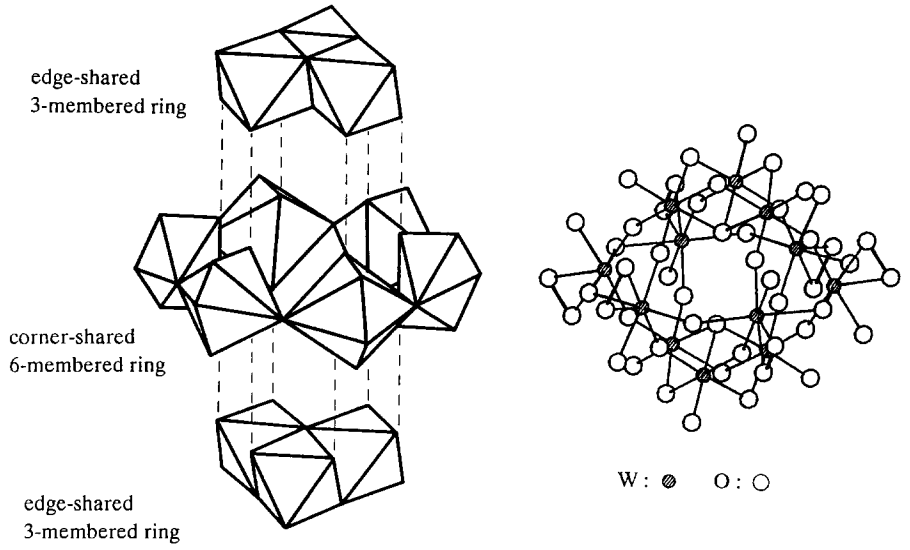

FIG. 8. Structural model of W-PTA.

4. *Structural Model*

Several crystals of tungsten oxides and its hydrates were examined on RDF but we could not find out the one that was appropriate. We also investigated polytungstates, $[K(C_{12}H_{24}O_6)]_4(CW_{12}O_{40}) \cdot 2H_2O$(*4*), $K_6[W_4O_8(O_2)_6(CO_3)] \cdot 6H_2O$ (*9*), etc., and Ba^{2+}, Cs^+ salts of W-PTA, Ba_xWO_3, and Cs_xWO_3 (*3*). The calculated RDFs are shown in Fig. 6, together with the observed ones for the as-prepared W-PTA and the sample No. 4 heated at 200°C. In these calculated RDFs the atomic contributions from K, C, H, Ba, Cs, and from O not bounded with W were neglected. At first we assumed that W-PTA had the same structure as the Keggin type $(W_{12}O_{40})^{8-}$ because the K^+ 18-crown-6 salt of WC-PTA had such a structural unit (*10*). The peak positions in the calculated RDF, however, were not consistent with the observed ones in W-PTA. On the contrary, the RDF calculated from the Ba^{2+} salt showed good agreement with those of the heat-treated samples. We consequently concluded that the framework structure in the heat-treated samples was similar to that of the Ba^{2+} salt, whose structure was based on three-, four-, and six-membered rings formed by WO_6 octahedra. As for the as-prepared W-PTA, we could not discover the appropriate tungstate.

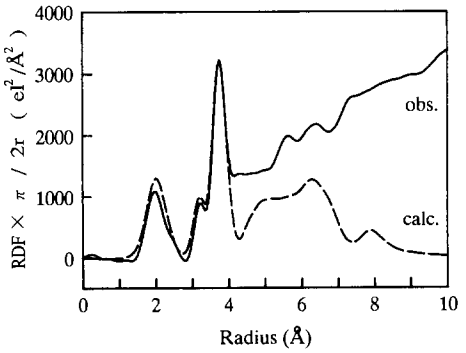

FIG. 9. Observed RDF of W-PTA (solid line) and calculated RDF from the proposed structural model (broken line).

We finally made a model based on "Paratungstate-B" with the formula, $[W_{12}O_{42}H_2]^{10-}$ (*11*), the structure of which is illustrated in Fig. 7. Three-membered octahedra are located at the upper and lower sides sharing each edge. These units are also

present in the Keggin structure. The other octahedra at the left and right sides share their edges. The upper/lower octahedra and left/right ones are joined by sharing their corners. In Paratungstate-B the ratio of the corners to edges shared was 7/5 and the observed ratio of W-PTA was about 3/1. Therefore, some modifications are needed. We then constructed the model shown in Fig. 8. The side edge-shared octahedra in paratungstate-B were replaced with a six-membered ring in which WO_6 octahedra were linked through their diagonal. Furthermore, WO_7 pentagonal bipyramids were substituted for the side octahedra to introduce peroxo groups. The upper and lower octahedra were joined in the same manner as those of Paratungstate-B. The chemical formula of this model polyanion was $[W_{12}O_{38}(O_2)_6]^{16-}$. The calculated RDF from this model showed good agreement with the observed one up to $R = 4$ Å, as shown in Fig. 9.

We did not consider the relations and interatomic contributions between the polyanions so that the RDF in $R > 4$ Å were unable to reproduce the observed pattern. We assumed that the nonbridging oxygen at the surface of this cluster (polyanion) model consisted of terminal W=O, H_2O, and peroxo groups, and these clusters were connected with hydrogen-bonding, such as W=O . . . H_2O–W and W–OH_2 . . . OH_2 . . . O=W.

Summary

The structure of W-PTA, which was prepared from metallic W and an aqueous solution of H_2O_2, was investigated using IR, Raman, and XRD. From the spectroscopic studies, it was suggested that W-PTA contains peroxo groups and terminal W=O bonds, and that it has structural units consisting of WO_6 octahedra and WO_7 pentagonal bipyramids. From the diffraction studies, it was found that W-PTA consisted of microclusters (polyanions), in which the networks were formed with corner-shared and edge-shared WO_6 and WO_7 polyhedra. The peroxo groups and the edge-shared polyhedra decreased and finally disappeared as the heat-treatment temperature became higher.

A Keggin-type structure was assumed but it was found that this structure was not suitable for W-PTA. We suggested a model which was constructed from three-membered WO_6 sharing their edges and a ring formed with six-membered WO_7 sharing their corners.

References

1. K. YAMANAKA, H. OKAMOTO, H. KIDOU, AND T. KUDO, *Japan. J. Appl. Phys.*, **25,** 1420 (1986).
2. T. KUDO, H. OKAMOTO, K. MATSUMOTO, AND Y. SASAKI, *J. Solid. State. Chem.* **66,** 283 (1987).
3. T. KUDO, A. KISHIMOTO, J. OI, AND H. INOUE, *Solid State Ionics*, in print.
4. K. MATSUMOTO, Y. OZAWA, Y. SASAKI, T. KUDO, AND H. OKAMOTO, *Inorg. Chim. Acta* **159,** 185 (1989).
5. M. F. DANIEL, B. DESBAT, J. C. LASSEGUES, B. GERANS, AND M. FIGLARZ, *J. Solid State Chem.* **67,** 235 (1987).
6. W. P. GRIFFITH, AND T. D. WICKINS, *J. Chem. Soc. (A)*, 397 (1968).
7. W. B. E. FREDERICK, AND R. P. BRUCE, *Acta Crystallogr.* **17,** 1127 (1964).
8. T. NANBA AND I. YASUI, *J. Solid State Chem.* **83,** 304 (1989).
9. R. STOMBERG, *Acta Chem. Scand. A* **39,** 507 (1985).
10. J. F. KEGGIN, *Proc. R. Soc. London, Ser. A* **144,** 75 (1934).
11. M. T. POPE, "Heteropoly and Isopoly Oxometalates," P. 50, Springer–Verlag, New York, (1983).